Properties of Water in Prestretched Recast Nafion

ARTICLE *in* MACROMOLECULES · JUNE 2008

Impact Factor: 5.8 · DOI: 10.1021/ma800194z

5 AUTHORS, INCLUDING:

Ryszard Wycisk
Vanderbilt University
71 PUBLICATIONS **930** CITATIONS
SEE PROFILE

Peter N Pintauro
Vanderbilt University
145 PUBLICATIONS **2,524** CITATIONS
SEE PROFILE

Properties of Water in Prestretched Recast Nafion

Jun Lin,[†] Pin-Han Wu,[†] Ryszard Wycisk,[†] Peter N. Pintauro,*[,†] and Zhiqing Shi[‡]

Department of Chemical Engineering, Case Western Reserve University, Cleveland, Ohio 44106, and Institute for Fuel Cell Innovation, National Research Council Canada, 3250 East Mall, Vancouver, British Columbia V6T IW5, Canada

Received January 27, 2008; Revised Manuscript Received March 29, 2008

ABSTRACT: Uniaxially prestretched recast Nafion membranes exhibited an unusual combination of properties (a proton conductivity equal to that of commercial Nafion but with a lower methanol permeability) which make them ideal candidates for use in a direct liquid methanol fuel cell. To better understand the function and underlying morphology of the prestretched membranes, water uptake and mobility data were collected and analyzed for draw ratios ranging from 1 to 7. Macroscopic (gravimetric) water uptake and the water self-diffusion coefficient (measured by NMR) were found to be invariant with membrane elongation and essentially identical to those measured in a commercial Nafion 117 film (a similar behavior was observed for proton conductivity). The ratio of freezable/nonfreezable water in prestretched recast Nafion, the water electro-osmotic drag coefficient, and the spin−lattice relaxation time constant of deuterated water, however, decreased with increasing film elongation, up to a draw ratio of 4. The functional dependence of these properties on draw ratio was similar to that observed for methanol permeability. The combined water results indicated that there were a greater number of smaller ionic/hydrophilic domains in prestretched recast Nafion as compared to commercial Nafion. Transmission electron microscopy of membrane cross sections confirmed this conclusion.

Introduction

The extent of water adsorption and the physical states of water in ionomeric membranes have been examined, using a variety of techniques, including macroscopic gravimetric and volumetric water uptake, NMR, infrared spectroscopy, radio tracer analyses, and dielectric relaxation spectroscopy.[1–8] The results of these studies are particularly important with regard to proton-exchange membranes that are used in hydrogen/oxygen and direct methanol fuel cells. The uptake and mobility of water within these ion-exchange membranes are intimately related to proton conduction, electro-osmotic drag, methanol permeability, and the film's mechanical properties.[9] There are numerous studies in the literature regarding water uptake and transport in Nafion perfluorosulfonic acid membranes[1–8] and in fuel cell membranes composed of sulfonated poly(arylene ether sulfone),[10] sulfonated poly(ether ether ketone),[11] and sulfonated polyimide.[12]

For the specific case of DuPont's Nafion, there is nanophase segregation of the nonpolar fluorinated (Teflon-like) backbone and the hydrophilic side chains (which terminate in sulfonic acid cation-exchange groups) prior to and during exposure to water. The hydrophilic domains in a fully hydrated film form an interconnecting proton conductive network with a characteristic dimension of ≈5 nm,[13] whereas the semicrystalline hydrophobic phase imparts mechanical strength to the membrane. Various models have been proposed to describe the nanomorphology of water-swollen Nafion, including a network of interconnecting water-filled inverted spherical micelles,[13,14] layered lamella,[15,16] rodlike structures,[17–19] and, more recently, inverted-micelle cylinders,[20] where the 5 nm dimension corresponds to the diameter of the cylindrical or the distance between lamella sheets. Within Nafion's hydrophilic domains, researchers have broadly identified two states of water:[21] (i) freezable water that interacts weakly or not at all with the polymer and exhibits freezing/melting transitions in a differential scanning calorimetry experiment and (ii) nonfreezing water that is strongly bound to ionic groups associated with the polymer.

The present paper deals with the measurement and interpretation of water uptake and mobility in uniaxially prestretched recast Nafion membranes. Prestretched membrane samples with a draw ratio between 4 and 7 exhibited unusual, but highly desirable, properties for direct methanol fuel cell (DMFC) applications, namely a high proton conductivity (the proton conductivity was the same as commercial Nafion and independent of draw ratio) and low methanol permeability (≈2.5 times lower than that in commercial Nafion for a draw ratio ≥4). Figure 1 shows the conductivity and methanol permeability properties of a 60 μm thick prestretched recast Nafion film relative to commercial Nafion 117, where the through-plane conductivity of water-equilibrated films at 25 °C and the permeability for 1.0 M methanol at 60 °C are plotted against the membrane draw ratio (which is defined as the ratio of the stretched membrane length to the original sample length). DMFC power densities with prestretched recast Nafion (draw ratio of 4) were 50% higher than those with commercial Nafion 117, at 60 °C with 1.0 M methanol and ambient pressure air.[22] The key innovative membrane fabrication steps were film

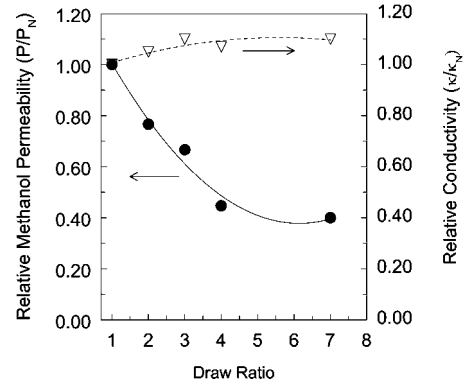

Figure 1. Through-plane proton conductivity (water-equilibrated membranes at 25 °C) and methanol permeability (1.0 M methanol at 60 °C) as a function of draw ratio for unstretched (draw ratio = 1) and prestretched recast Nafion. κ_N and P_N are the proton conductivity and methanol permeability of commercial Nafion 117 (κ_N = 0.10 S/cm; $P_N = 3.6 \times 10^{-6}$ cm^2/s).

* Corresponding author: Ph 216.368.4150; Fax 216 0.368.3016; e-mail pnp3@case.edu.
[†] Case Western Reserve University.
[‡] National Research Council Canada.

10.1021/ma800194z CCC: $40.75
Published on Web 05/17/2008

stretching prior to polymer annealing and annealing the film under tension.[22] Film elongation without annealing or annealing prior to stretching did not produce a membrane with good DMFC properties. Without annealing, recast membranes lacked the requisite mechanical properties and stretched recast membranes retracted to their original shape after a few hours of exposure to a hot methanol solution if film elongation were carried out after polymer annealing. (This retraction behavior was also observed when a commercial Nafion 117 film was uniaxially stretched.) Here, we describe our membrane material as "prestretched recast Nafion" to better characterize the fabrication process; in a prior publication[22] it was referred to as "stretched recast Nafion."

We report here on experimental results from a series of water sorption/transport experiments: macroscopic equilibrium water uptake, low-temperature differential scanning calorimetry of water-equilibrated films, water self-diffusion coefficient as determined by pulsed field gradient NMR, spin−lattice relaxation time of deuterated water, and the measurement of the electro-osmotic drag coefficient of protons in fully hydrated prestretched recast films. The water data were combined with transmission electron micrographs of membrane cross sections. Collectively, the experimental results provide important insights into the nanomorphology of prestretched recast Nafion and the interaction of water molecules with the membrane, which in turn shed light on the performance properties of such films when they are used in a direct methanol fuel cell.

Experimental Section

Membrane Preparation. Membranes were prepared from Nafion polymer that was recovered after evaporating the solvent from a commercial Nafion solution (Liquion 1115 from Ion Power, Inc.). The dried Nafion material was fully dissolved in dimethylacetamide (DMAc) at room temperature, and membranes were cast in a Teflon dish from the resulting 10 wt % solution. DMAc solvent was partially evaporated at 60 °C, resulting in a 200−400 μm thick film that contained 10−15 wt % DMAc. After the DMAc-swollen membrane was removed from the casting surface, it was placed in the stretching frame, heated to 125 °C, and then uniaxially stretched to a desired draw ratio. The membrane was kept in the stretching frame and heating was continued at 125 °C for 1 h to fully evaporate DMAc, followed by an annealing step at 150 °C for 2 h. The membrane was removed from the stretching apparatus, boiled in 1.0 M H_2SO_4 for 1 h, and then boiled in deionized water for 1 h. Prestretched recast membranes (with a wet thickness of 60−90 μm) were stored in room temperature water until further use.

Equilibrium, Macroscopic Water Uptake. Equilibrium absorption of deionized water in membrane samples was determined at room temperature. The wet mass (W_{wet}) was measured immediately after removing residual water from the film surfaces. Membrane dry mass (W_{dry}) was obtained after drying at 120 °C for 1 h. Water uptake, presented as the number of water molecules per sulfonic acid site, was calculated from

$$\lambda(H_2O/SO_3^-) = \left[\frac{W_{wet} - W_{dry}}{W_{dry}}\right] \frac{1}{[IEC]\,[MW_w]} \qquad (1)$$

where IEC denotes the membrane ion-exchange capacity (0.909×10^{-3} mol/g for Nafion) and MW_w is the molecular weight of water (18 g/mol).

Differential Scanning Calorimetry (DSC). Low-temperature DSC experiments were performed using a Mettler Toledo DSC822e configured with an intracooler capable of reaching temperatures of −70 °C. Fully hydrated membrane samples were carefully blotted to remove surface water and then transferred immediately to sealed aluminum pans. The samples were quickly placed in the calorimeter and cooled to −60 °C. The samples were then heated to 50 °C at a rate of 5 °C/min. The water melting endotherms were integrated to calculate the amount of freezable water in a sample, based on the heat of fusion for bulk water. The weight percentage of freezable water in a given membrane, as compared to the total water content in the sample, was calculated using the following equation:

$$\%\ \text{freezable water} = \frac{\Delta H}{\Delta H_f} \frac{1+\beta}{\beta} \times 100\% \qquad (2)$$

where ΔH is the integrated enthalpy from the DSC melting endotherm based on the total sample mass, ΔH_f is the heat of fusion for bulk water (334 J/g),[23] and β is the gravimetric water uptake of the sample ($\beta = m_w/m_d$, where m_w and m_d are the total mass of water in a membrane sample and the dry mass of that sample, respectively).

NMR Measurement. NMR data were collected using a Bruker Avance 400 MHz wide-bore spectrometer with microimaging capability. After blotting the surface water from a water-equilibrated membrane sample, the hydrated film was quickly rolled into a cylinder (10 mm diameter and 5 cm length) and placed in a clean and dry NMR tube within which the hydration condition of the membrane could be maintained. The self-diffusion coefficient of water was measured using the pulsed-field gradient spin−echo (PFG-SE) method.[24] The ^2H spin−lattice relaxation time (T_1) was measured by inversion−recovery sequences.[1,25] The maximum gradient strength was calibrated with water and found to be 96.0 G cm^{-1}. All measurements were made at 25 °C.

Electro-osmotic Drag of Water. The electro-osmotic drag coefficient in commercial and prestretched recast Nafion membranes was measured using the procedure reported in the literature by Ren and Gottesfeld.[26] Membrane-electrode assemblies (MEAs) with a geometric electrode area of 5.0 cm^2 and anode/cathode catalyst loadings of 4.0 mg/cm^2 were prepared from membrane samples using a method described elsewhere.[22] An MEA was loaded into a fuel cell test fixture (with single anode and cathode serpentine flow channels) and operated at high current densities (≥200 mA/cm^2, so that the electromigration of water from the anode to the cathode far exceeded any back diffusion of water). The methanol concentration and flow rate were 1.0 M methanol and 1.5 mL/min, respectively, and the cathode gas feed was dry oxygen at a flow rate of 250 sccm. A back-pressure of 1.72×10^5 Pa was applied to both the anode and cathode to minimize/eliminate water transport due to a hydraulic pressure difference across the membrane. Water in the cathode oxygen exhaust was trapped in a Schwartz U-shaped drying tube containing Drierite (W.A. Hammond Drierite Co. Ltd.). The methanol crossover flux during current flow was found by measuring the carbon dioxide concentration in the cathode oxygen exhaust stream (after water was removed in the U-tube), using a calibrated Vaisala GMM12B or GMM220A CO_2 detector. The water flux due to electro-osmotic drag was calculated by subtracting the water produced by the primary cathodic oxygen reduction reaction (as determined from the current density and electrode area) and the water generated by methanol oxidation at the cathode as a consequence of methanol crossover (as determined from the concentration of CO_2 in the oxygen exhaust and the oxygen flow rate) from the total water flux as determined by the mass of water trapped in the U-tube for a given time period. From the applied constant current density and the flow rate of water transported across the membrane per unit time, the electro-osmotic drag coefficient (with units of H_2O/H^+) was calculated.

Transmission Electron Microscopy. Samples for transmission electron microscopy (TEM) examination were prepared using the following steps: (1) membrane samples, 1 mm × 5 mm in size, were stained by soaking for 12 h in a saturated lead acetate solution; (2) the samples were rinsed thoroughly with deionized water and then dried under vacuum at 60 °C for 2 h; (3) the membranes were embedded in a block template using Spurr's epoxy resin and cured at ∼60 °C for ca. 12 h; (4) the blocks were sectioned to yield slices 50−75 nm in thickness, using a Leica Ultracut ultramicrotome; and (5) the slices were collected on copper grids. Images were obtained using a Hitachi H7600 transmission electron microscope with an accelerating voltage of 80 kV.

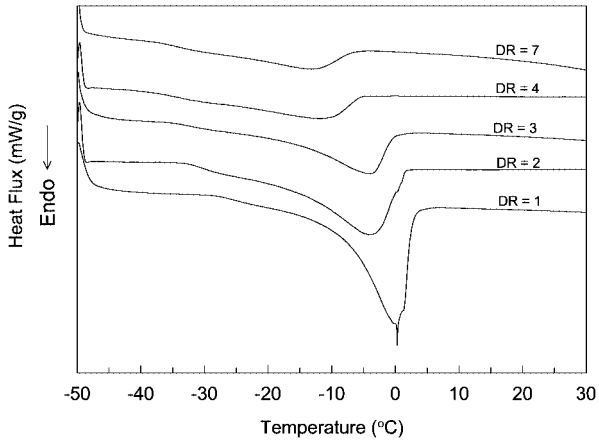

Figure 2. Low-temperature differential scanning calorimetry thermograms of water-equilibrated unstretched (draw ratio = 1) and prestretched recast Nafion (DR denotes draw ratio).

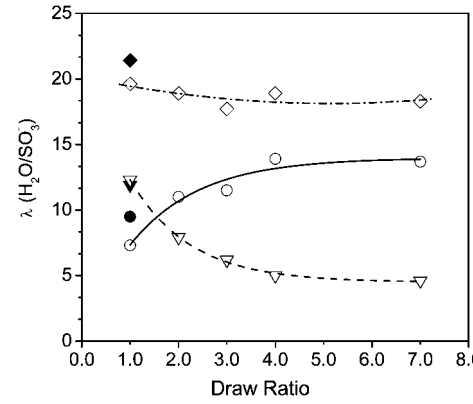

Figure 3. Total (◇), freezable (▽), and nonfreezable (○) water content of commercial Nafion 117 (closed symbols) and recast Nafion (open symbols): unstretched recast Nafion (draw ratio = 1) and prestretched recast Nafion membranes at different draw ratios.

Results and Discussion

Equilibrium (macroscopic) gravimetric water uptake (swelling) at 25 °C for prestretched recast Nafion was essentially constant at 19 H_2O/SO_3^- (30 wt % uptake), independent of draw ratio (for draw ratios of 2−7) and slightly lower than that measured for commercial Nafion 117 ($\lambda = 21$). Uniaxial film elongation often leads to an increase in crystallinity of semicrystalline polymers.[27,28] If the prestretched films were substantially more crystalline, then there might be a reduction in water uptake (crystallites would act as physical cross-links that would limit membrane swelling). The measured water uptake results and preliminary X-ray diffraction data,[22] however, indicate that the increase in crystallinity upon membrane elongation was small and did not affect the water swelling behavior of the prestretched recast Nafion films.

Low-temperature DSC water-melting endotherms for unstretched (draw ratio of 1) and prestretched recast Nafion (draw ratio of 2−7) are shown in Figure 2. The data were used to elucidate the different types of water (freezable vs nonfreezable) in fully hydrated membrane samples. The most striking feature of these plots is the monotonic decrease in the size of the water melting peak with increasing draw ratio. Clearly, there is less freezable water in Nafion upon prestretching a recast film. (Although not shown in Figure 2, the water endotherm for Nafion 117 was almost identical to that for unstretched recast Nafion.) There was also a depression in the temperature at which the freezable water melted in the prestretched Nafion samples. Whereas thermograms of unstretched Nafion revealed the presence of a sharp endothermic component at 0 °C, indicating the existence of water with bulklike properties, freezable water in prestretched recast Nafion melted at a temperature below 0 °C (e.g., about −10 °C for a draw ratio of 4). This result is qualitatively similar to what others have found in partially swollen Nafion. For example, Siu et al.[21] reported on a 10 °C depression of the melting point for water in a commercial Nafion 117 membrane that was equilibrated with 95% RH air, where $\lambda = 11-14$ and where the membrane sulfonic acid concentration (based on the total volume of water in the membrane) before freezing was about 1.4 M, as compared to 1.1 M for a membrane fully swollen with liquid water. In the present study, the melting point temperature depression for fully hydrated prestretched Nafion (total $\lambda = 19$) was associated with morphological changes in the membrane polymer, rather than fixed-charge concentration effects, as will be discussed in more detail below.

Plots of the total, freezable, and nonfreezable water (given as the number of water molecules per sulfonic acid site) in Nafion 117 and unstretched and prestretched recast Nafion (for draw ratios of 2−7) are shown in Figure 3, with $\lambda_{nonfreeze} = \lambda_{total} - \lambda_{freeze}$ (where λ_{freeze} was determined from the data in Figure 2). The value of 12 for λ_{freeze} in a water-equilibrated Nafion 117 membrane is comparable to that reported in the literature ($\lambda_{freeze} = 9$ in ref 21). As can be seen, there is a steady and substantial decrease in the amount of freezable water in recast Nafion as it is elongated, up to a draw ratio of 4. In commercial Nafion 117 and unstretched recast Nafion (draw ratio of 1), ~60% of the total membrane water freezes, whereas only 26% of the water freezes in prestretched recast Nafion (draw ratio equal to or greater than 4). The plateau in the freezable water content for draw ratios ≥4 cannot be explained at the present time. The general shape of the freezable water content vs draw ratio curve, however, does mirror the dependence of methanol permeability on film elongation (Figure 1). This result is consistent with prior studies, which concluded that methanol permeability in proton exchange membranes is a function of the membrane's freezable water content.[10] The increase in $\lambda_{nonfreeze}$ with draw ratio in Figure 3 and the depression in the water melting temperature (Figure 2) were tentatively associated with a water confinement phenomenon, where the size of the hydrophilic domains decreased with increasing draw ratio, and possibly electrostatic water polarization/alignment effects, where there was more efficient and extensive hydration of membrane fixed-charges when Nafion was elongated.

The data in Figures 2 and 3 suggest that there was a redistribution of ionic domains in prestretched Nafion, where the domain size decreased and the number of domains increased (to maintain constant total water uptake) with increasing draw ratio. To confirm this hypothesis, transmission electron micrographs of prestretched recast Nafion membrane cross sections were collected. The TEM results are shown in Figure 4, where the membrane cross sections are perpendicular to the stretching direction (i.e., stretching was perpendicular to the $x-y$ plane of the page). The size of the ionic domains (darkened regions in Figure 4) was smaller and the number of such domains increased with increasing film elongation. Additionally, both the size and distribution of the ionic domains in the prestretched films were highly uniform (i.e., water was spread out more uniformly in prestretched recast Nafion). The decrease in domain size for a high draw ratio was significant; at a draw ratio of 7, for example, the ionic (hydrophilic) domain dimension was ~2 nm, as compared to about 8 nm for an unstretched recast film. Although the TEMs are of dry membrane samples, the general morphology should be preserved upon exposure to water,[29] with an increase in both stretched and nonstretched domain size upon water sorption. Further investigations are necessary to fully

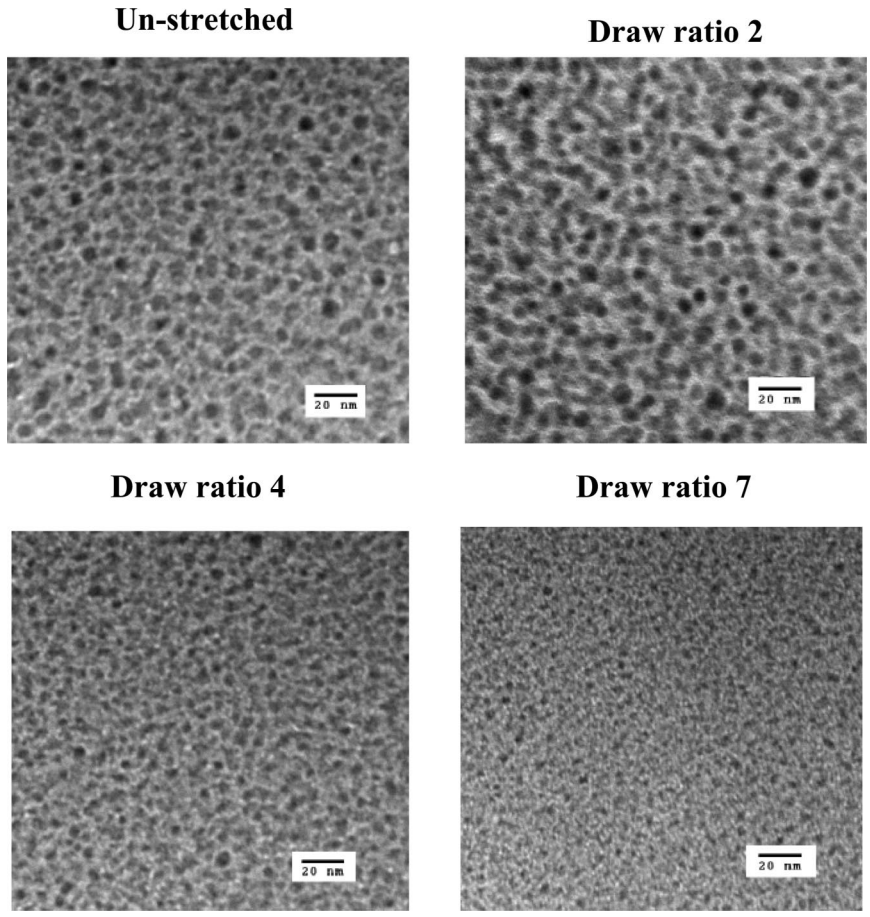

Figure 4. Transmission electron micrographs of unstretched (draw ratio = 1) and prestretched recast Nafion membrane cross sections. Dark regions are the hydrophilic domains (stretching direction was perpendicular to the $x-y$ plane of the page).

understand the nanomorphology of prestretched recast Nafion. For example, additional TEM studies of membrane cross sections parallel to the stretching direction are needed, along with small-angle X-ray scattering (SAXS) measurements in the three orthogonal planes of the membrane. Such experiments are planned and will be the subject of a future publication.

Within experimental accuracy, the water self-diffusion coefficient was constant in commercial Nafion 117 (8.20×10^{-6} cm^2/s), unstretched recast Nafion (8.33×10^{-6} cm^2/s), and prestretched recast Nafion films of varying draw ratios (8.35×10^{-6} for draw ratios of 2−7), as measured by pulsed-field-gradient NMR. These diffusion coefficients were similar to data in the literature for a liquid water equilibrated Nafion 117 film (7.5×10^{-6} cm^2/s, from ref 1). The water diffusion coefficient in Nafion is smaller than that in bulk water (2.13×10^{-5} cm^2/s), reflecting the highly tortuous diffusion pathway for water in a low-porosity membrane (Nafion swelling is ≈30% in water). One would anticipate a correlation between the average mobility of a water molecule in prestretched recast Nafion and the freezable water content, if the mobilities of freezable and nonfreezable species were significantly different, and thus, a plot of water self-diffusion coefficient vs draw ratio should be similar in shape to the freezable water content plot in Figure 3. Unexpectedly, there was no change in the self-diffusion coefficient of water with draw ratio. This indicated either that the exchange rate between freezable and nonfreezable water molecules was faster than the NMR acquisition time or that the thermal characteristics of the water of hydration did not reflect its actual translational dynamics. To further investigate the above finding, the ^{2}H spin−lattice relaxation time of deuterated water (T_1) in prestretched Nafion samples was measured and found to decrease with draw ratio (see Figure 5), indicating slower

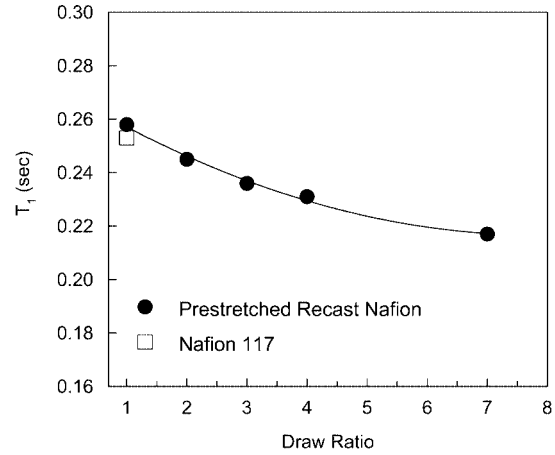

Figure 5. Spin−lattice relaxation time of deuterated water (T_1) in commercial Nafion 117, unstretched recast Nafion (draw ratio = 1), and prestretched recast Nafion at different draw ratios.

rotational motion and a higher viscosity of water upon film elongation. The value of T_1 at a draw ratio of 7 (0.22 s) was half that of bulk water (0.45 s)[1] and very close to that seen in commercial Nafion 117 under reduced swelling conditions (T_1 = 0.21 s at 100% RH, where λ = 14)[1] where there was significant contraction of the membrane's ionic domains. Thus, the T_1 data are in qualitative agreement with the DSC results; i.e., this particular property of water in prestretched recast Nafion (draw ratio ≥4) is similar to that in a commercial Nafion film at low water content. One explanation for the invariance in water self-diffusion coefficient with Nafion elongation is a decrease in the tortuosity of hydrophilic domains with draw ratio, which

compensates for a reduction in water mobility. The pulsed-field-gradient NMR method of determining water self-diffusion coefficient involves the measurement of water movement on the length scale of microns for diffusion coefficients of the magnitude reported here and, thus, is reflective of both the membrane tortuosity and water mobility.

In light of the DSC and NMR results for water in prestretched recast Nafion and the supporting evidence provided by the TEM images in Figure 4, a discussion of proton conductivity (constant conductivity with draw ratio, as shown in Figure 1) in relation to membrane morphology is warranted. Numerous studies with commercial Nafion membranes have shown that proton conductivity decreases with decreasing total water content, where the amount of sorbed water was varied by equilibrating a membrane sample with humidified air at a water activity <1. For example, Gavach et al.[30] found that the conductivity of perfluorosulfonic acid membranes increased significantly when the average number of water molecules per sulfonic acid site was >6. (In that study it was assumed that $\lambda = 6$ represents the minimum number of water needed to create a primary hydration shell on the SO_3H ion-exchange groups and to generate a continuous, percolating water of hydration phase.) When Nafion 117 was equilibrated in 95% RH air at 25° (where $\lambda = 12$), the proton conductivity at 25 °C was ≈0.06 S/cm vs 0.09−0.10 S/cm for a liquid water-equilibrated film.[1] Thus, the data in Figures 1 and 3 (total water content results) for prestretched recast Nafion are consistent with our general understanding of proton mobility in Nafion (i.e., the high total water content of prestretched recast Nafion, for all draw ratios, translates into a high proton conductivity).

The interpretation of the conductivity data in terms of the freezable/nonfreezable water contents in Figure 3 is more complex. Clearly, proton conductivity is not dependent on the amount of freezable water in prestretched recast Nafion. Such behavior has never been observed before in a proton conducting fuel cell membrane like Nafion because it was not possible to reduce the freezable water content without also lowering the total amount of sorbed water. It has generally been thought that proton conductivity in Nafion scales directly with freezable water content, since the presence of bulklike water increases proton mobility in fully hydrated membranes.[21] The results in Figures 1 and 3 contradict this generally held belief. Thus, a prestretched recast Nafion film with as little as 2/5 the amount of freezable water as compared to Nafion 117 (i.e., $\lambda_{freeze} = 5$ at a draw ratio of 4) maintains its high proton conductivity. The combined DSC, water diffusivity, and conductivity results suggest that (i) there is a decrease in the tortuosity of the water-filled pore network in prestretched recast Nafion that compensates for less freezable water and a lower local proton mobility and/or (ii) there is a different proton conduction mechanism in the water-filled pores of prestretched recast Nafion. In fact, theoretical studies indicate that proton hopping can occur via water bridging between two sulfonic groups if they are sufficiently close to one another.[31–33] Smaller ionic/hydrophilic domains in prestretched Nafion should result in closer spacing of sulfonic groups which could promote pore surface diffusion via a proton hopping mechanism. The interesting and unique proton conductivity behavior of prestretched recast Nafion vis-à-vis its membrane water properties has important implications for hydrogen/oxygen fuel cells. For example, the results imply that the proton conductivity in a highly prestretched recast Nafion film (draw ratio ≫7) containing no freezable water will remain high when exposed to low-humidity environments (although it is not clear how one might create such a film in light of the plateau in the freezable water content with draw ratio in Figure 3). The total water content in such a Nafion membrane should be similar to that of commercial Nafion, with all of the water in a nonfreezable (and presumably nonevaporative) state. Such membrane fabrication experiments should be coupled to studies on the split of freezable/nonfreezable water in prestretched recast Nafion of various draw ratios, as a function of temperature and water vapor activity.

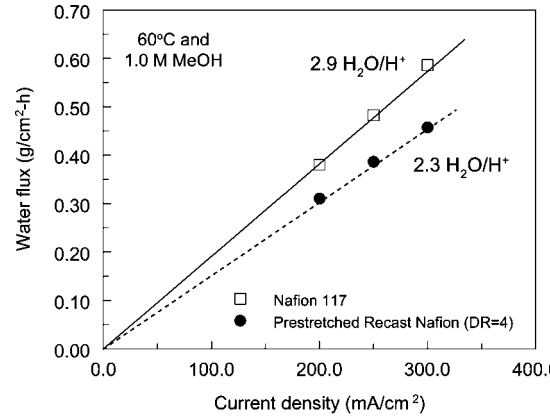

Figure 6. Electro-osmotic water flux as a function of current density for commercial Nafion 117 and prestretched recast Nafion (draw ratio of 4). $T = 60$ °C.

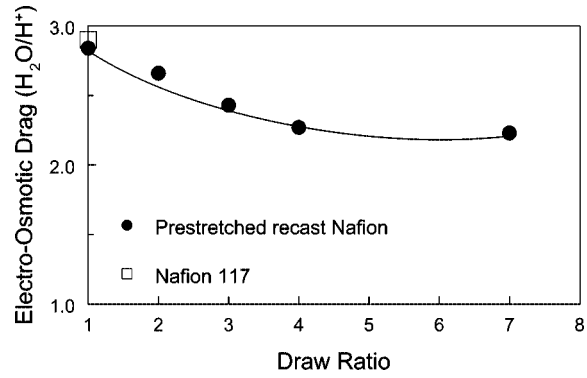

Figure 7. Electro-osmotic water drag coefficient of commercial Nafion 117, unstretched recast Nafion (draw ratio = 1), and prestretched recast Nafion of different draw ratios.

The final set of experiments for elucidating the properties of water in prestretched recast Nafion was the determination of electro-osmotic water drag coefficient (defined as the number of water molecules per H^+ that move through the membrane under the influence of an applied electric field). These data were collected in a modified direct liquid methanol fuel cell experiment, as described above. The water flux solely associated with proton transport is plotted against current density (which is proportional to the transmembrane proton flux) in Figure 6 for commercial Nafion 117 and a prestretched recast Nafion sample with a draw ratio of 4. The straight line behavior of the data with a zero intercept indicated that the electro-osmotic drag coefficient of water was independent of current density and could be calculated from the slopes of these lines. A plot of this parameter as a function of draw ratio for a series of prestretched recast Nafion membranes is shown in Figure 7. As expected, the water drag coefficient in prestretched Nafion was lower than that in commercial Nafion (10−25% lower) and decreased with increasing draw ratio. This may be the result of the increased viscosity of pore water, revealed by the T_1 experiments, which promotes more compact proton solvation vehicles and possibly a proton hopping mechanism (as discussed previously) where bare protons are transported through structured (frozen) water along the pore surface. A decrease in the electro-osmotic drag coefficient should, to a certain extent, retard methanol permeability in an operating fuel cell. The measured

methanol permeabilities in Figure 1, however, cannot be linked directly to the reduction in the electro-osmotic drag coefficient. Other mechanisms of methanol blocking are probably operating, including partitioning effects, but these require further studies.

Conclusions

Uniaxially prestretched recast Nafion membranes exhibit unusual proton conductivity and methanol permeability behavior (a proton conductivity that is independent of draw ratio and a methanol permeability that decreases with elongation up to a draw ratio of 4), which make them ideal candidates for use in a direct liquid methanol fuel cell. To better understand the underlying morphology of these membranes, water uptake and mobility data were measured and analyzed for draw ratios ranging from 1 (unstretched) to 7. A series of macroscopic (gravimetric) water uptake, low-temperature differential scanning calorimetry, NMR, and electro-osmotic drag coefficient experiments were performed on water-equilibrated membrane samples. Macroscopic water uptake and the water self-diffusion coefficient were found to be invariant with membrane draw ratio and essentially identical to those measured in a commercial Nafion 117 film. The amount of freezable water in prestretched recast Nafion, however, decreased and the amount of nonfreezable water increased with increasing film elongation (up to a draw ratio of 4). Thus, at a draw ratio of 4, the split between freezable and nonfreezable water was $\lambda_{freeze} = 5$ and $\lambda_{nonfreeze} = 13.9$, as compared to $\lambda_{freeze} = 12.3$ and $\lambda_{nonfreeze} = 7.3$ for unstretched recast Nafion and $\lambda_{freeze} = 11.9$ and $\lambda_{nonfreeze} = 9.5$ for commercial Nafion 117. The fact that proton conductivity is independent of the freezable water content in prestretched recast Nafion is a new and important result of this study, with potentially important and far-reaching implications with regards to the mechanism of proton transport in such films and the use of prestretched recast Nafion in a hydrogen/air fuel cell at low-humidity conditions. The NMR results (a T_1 relaxation time that decreased with elongation but a water self-diffusion coefficient that was independent of film stretching and freezable water content) imply that the hydrophilic water network is less tortuous in a prestretched film.

The DSC results (a greater fraction of the sorbed water in prestretched Nafion was nonfreezable as compared to commercial Nafion) and the macroscopic water swelling data (the total water uptake in prestretched and commercial Nafion were essentially the same) suggest a new nanomorphology for prestretched recast Nafion where there is a decrease in the size and increase in the number of hydrophilic water-swollen domains, up to a draw ratio of 4. This structure was confirmed by TEM images of prestretched recast Nafion cross sections at various draw ratios.

Methanol permeability, the spin−lattice relaxation time constant of deuterated water (T_1), and the electro-osmotic drag coefficient of protons in prestretched recast Nafion all decreased with increasing draw ratio and mirrored the variation of freezable water content with film elongation. Thus, less freezable (and more nonfreezable) water in a prestretched Nafion film translates into a high average viscosity for membrane-phase water, which in turn decreases the number of water molecules that are dragged with protons. The dependence of methanol permeability on film elongation is consistent with prior studies which concluded that methanol permeability in proton exchange membranes is a function of the membrane's freezable water content. One explanation to reconcile the different dependencies of water self-diffusion coefficient and methanol permeability (the product of partition coefficient and diffusion coefficient) on draw ratio (i.e., freezable water content) is that methanol partitioning at the membrane/solution interface is reduced in prestretched recast films, with very little change in methanol diffusion coefficient, but this requires further studies.

References and Notes

(1) Zawodzinski, T. A., Jr.; Derouin, C.; Radzinski, S.; Sherman, R. J.; Smith, V. T.; Springer, T. E.; Gottesfeld, S. *J. Electrochem. Soc.* **1993**, *140*, 1041–1047.
(2) Zawodzinski, T. A., Jr.; Springer, T. E.; Davey, J.; Jestel, R.; Lopez, C.; Valerio, J.; Gottesfeld, S. *J. Electrochem. Soc.* **1993**, *140*, 1981–1985.
(3) Chen, R. S.; Jayakody, J. P.; Greenbaum, S. G.; Pak, Y. S.; Xu, G.; McLin, M. G.; Fontanella, J. J. *J. Electrochem. Soc.* **1993**, *140*, 889–895.
(4) Zawodzinski, T. A., Jr.; Neeman, M.; Sillerud, L. O.; Gottesfeld, S. *J. Phys. Chem.* **1991**, *95*, 6040–6044.
(5) Moilanen, D. E.; Piletic, I. R.; Fayer, M. D. *J. Phys. Chem. A* **2006**, *110*, 9084–9088.
(6) Pintauro, P. N.; Bennion, D. N. *Ind. Eng. Chem. Fundam.* **1984**, *23*, 234–243.
(7) McLin, M. G.; Wintersgill, M. C.; Fontanella, J. J.; Chen, R. S.; Jayakody, J. P.; Greenbaum, S. G. *Polym. Mater. Sci. Eng.* **1993**, *68*, 119.
(8) Polizos, G.; Lu, Z.; Macdonald, D. D.; Manias, E. *Mater. Res. Soc. Symp. Proc.* **2007**, *972*, 131–136.
(9) Hickner, M. A.; Ghassemi, H.; Kim, Y. S.; Einsla, B. R.; McGrath, J. E. *Chem. Rev.* **2004**, *104*, 4587–4612.
(10) Kim, Y. S.; Dong, L.; Hickner, M. A.; Glass, T. E.; Webb, V.; McGrath, J. E. *Macromolecules* **2003**, *36*, 6281–6285.
(11) Kreuer, K. D. *J. Membr. Sci.* **2001**, *185*, 29–39.
(12) Piroux, F.; Espuche, E.; Mercier, R.; Pinéri, M. *J. Membr. Sci.* **2003**, *223*, 127–139.
(13) Gierke, T. D.; Munn, G. E.; Wilson, F. C. *J. Polym. Sci., Polym. Phys. Ed.* **1981**, *19*, 1687–1704.
(14) Gebel, G.; Lambard, J. *Macromolecules* **1997**, *30*, 7914–7920.
(15) Starkweather, H. W., Jr. *Macromolecules* **1982**, *15*, 320–323.
(16) Litt, M. H. *Polym. Prepr.* **1997**, *38*, 80–81.
(17) Rollet, A.-L.; Diat, O.; Gebel, G. *J. Phys. Chem. B* **2002**, *21*, 3033–3036.
(18) Rubatat, L.; Rollet, A.-L.; Gebel, G.; Diat, O. *Macromolecules* **2002**, *35*, 4050–4055.
(19) Rubatat, L.; Gebel, G.; Diat, O. *Macromolecules* **2004**, *37*, 7772–7783.
(20) Schmidt-Rohr, K.; Chen, Q. *Nat. Mater.* **2008**, *7*, 75–83.
(21) Siu, A.; Schmeisser, J.; Holdcroft, S. *J. Phys. Chem. B* **2006**, *110*, 6072–6080.
(22) Lin, J.; Wycisk, R.; Pintauro, P. N.; Kellner, M. *Electrochem. Solid-State Lett.* **2007**, *1*, B19−B22.
(23) Hickner, M. A.; Fujimoto, C. H.; Cornelius, C. J. *Polymer* **2006**, *47*, 4238–4244.
(24) Stejskal, E. O.; Tanner, J. E. *J. Chem. Phys.* **1965**, *42*, 288–291.
(25) Haacke, E. M.; Brown, R. W.; Thompson, M. R.; Venkatesan, R. *Magnetic Resonance Imaging: Physical Principles and Sequence Design*; Wiley: New York, 1999; pp 129−134.
(26) Ren, X.; Gottesfeld, S. *J. Electrochem. Soc.* **2001**, *148*, A87−93.
(27) Binsbergen, F. L. *Nature (London)* **1966**, *211*, 516–517.
(28) Keller, A. *Faraday Discuss. Chem. Soc.* **1979**, *68*, 145–166.
(29) Rubatat, L.; Shi, Z.; Diat, O.; Holdcroft, S.; Frisken, B. J. *Macromolecules* **2006**, *39*, 720–730.
(30) Gavach, C.; Pamboutzouglou, G.; Nedyalkov, M.; Pourcelly, G. *J. Membr. Sci.* **1989**, *45*, 37–53.
(31) Eikerling, M.; Kornyshev, A. A. *J. Electroanal. Chem.* **2001**, *502*, 1–14.
(32) Roudgar, A.; Narasimachary, S. P.; Eikerling, M. *J. Phys. Chem. B* **2006**, *110*, 20469–20477.
(33) Thompson, E. L.; Capehart, T. W.; Fuller, T. J.; Jorne, J. *J. Electrochem. Soc.* **2006**, *153*−2362.

MA800194Z